

TWO-PHASE C-MEANS CLUSTERING WITH NOISE REDUCTION USING FUZZY RULES

K.Kadambavanam¹, T.Senthilnathan²

¹Associate Professor and Head, Department of Mathematics,
Sri. Vasavi College, Erode, Tamil Nadu, (India).

²Associate Professor, Department of Mathematics,
Erode Arts and Science College, Erode, Tamil Nadu, (India).

ABSTRACT

The objective of this paper is to develop an effective fuzzy clustering method for segmentation of images. The conventional fuzzy c-means clustering with spatial feature (FCM_S) and its variations have their own limitations if the images are corrupted by heavy noise. If noise exists in the spatial neighbourhood information, then it affects the clustering. This article proposes a new mask to provide better spatial information to overcome the above problem in clustering, using conventional fuzzy c means.

In the conventional defuzzification method used in fuzzy c-means clustering with spatial feature, there are two disadvantages. First, as the pixels' partition membership values are used to calculate the pixels' gray scale values, the noise less pixels' gray scale values are changed by the inference calculations. So the peak signal to noise ratio between the output data and the original (noise less) data is very low. Second, as the output image loses its sharpness, the non-Euclidian structures are not revealed well. For better performance, a new defuzzification method is proposed in this article. It presents algorithms for the proposed new mask, clustering, and the defuzzification. The main properties of the proposed method are illustrated by using synthetic, real, and magnetic resonance (MR) images. A quantitative evaluation of this method is also presented.

Keywords: Defuzzification, Filter Window, Fuzzy C-Means Clustering, Grey Value, Spatial Feature

I INTRODUCTION

Clustering is the process of dividing data elements into classes or clusters so that items in the same class are as similar as possible. In clustering research, many methods are invoked. The applications are in various engineering and scientific branches like medical image segmentation (Yong, *et al.* [1]), remote sensing, marketing, analysing public opinion about an issue, elections etc. (Pham, *et al.* [2], Bezdek, *et al.* [3], Wells, *et al.* [4]). But most of the clustering methods are crisp in which a data belongs to only one cluster. But in real life many cases are related to the fact that a pattern (or data) often cannot be thought of as belonging to a single cluster only. So, a description in which the membership of a pattern is shared among clusters is necessary. To rectify the problem of being crisp (Pham, *et al.* [5]), the fuzzy set theory, proposed by Zadeh [6] gives an effective method of soft clustering. The fuzzy c-means (FCM) clustering algorithm was first introduced by Dunn [7] and later extended by Bezdek [8]. Chen *et al.* [9] improved the fuzzy c means clustering by introducing kernel-induced metric, to reveal non-Euclidian structures in clustering. Ahmed *et al.* [10] incorporated spatial neighbourhood information into fuzzy c-means clustering to make it insensitive to noise in input image. But

these methods are having some disadvantages, that noise in spatial feature creeps into miss classification of data. Noiseless data are changed unnecessarily by the inference calculations in defuzzification. It results in blurred output image. In order to rectify these drawbacks, this paper introduces (i) a new mask to filter the noise in spatial information, (ii) a new clustering method based on the standard FCM, and (iii) a new defuzzification method.

II SOME BASIC TERMINOLOGIES

2.1 Fuzzy c-means clustering (FCM)

Bezdek [8] introduced the concept of fuzzy partition in order to extend the notion of membership of data to clusters. The FCM algorithm identifies clusters as fuzzy sets, in which each datum is assigned to partition membership in each cluster. It attempts to partition a set of N data $X = \{x_1, x_2, \dots, x_N\}$ where each $x_j \in \mathcal{R}^P$ into C ($2 \leq C \leq N$) fuzzy clusters based on some criterion. The algorithm returns a set of C cluster centers $V = \{v_1, v_2, \dots, v_C\}$ and a partition matrix $U = [u_{ij}]$, when $u_{ij} \in [0, 1]$, $i = 1, 2, \dots, C$, $j = 1, 2, \dots, N$. The element u_{ij} specifies the degree to which element x_j belongs to the cluster c_i .

A mathematical structure for the problem is

$$\text{minimize } J_m = \sum_{i=1}^C \sum_{j=1}^N u_{ij}^m \|x_j - v_i\|^2 \quad (1)$$

$$\text{subject to, } \sum_{i=1}^C u_{ij} = 1 \text{ for } j = 1, 2, \dots, N, \quad (2)$$

$$\text{and } 0 < u_{ij} < 1 \text{ for } i = 1, 2, \dots, C, j = 1, 2, \dots, N \quad (3)$$

where m – fuzziness of the resulting partition, ($1 \leq m \leq \infty$),

$\|x_j - v_i\|$ – the difference between x_j and v_i ($x_j, v_i \in \mathcal{R}^P$),

u_{ij} – partition membership of x_j in the cluster i ,

$v_i \in \mathcal{R}^P$ – prototype or centroids of the cluster i ,

N – number of data,

and C – number of clusters.

In image clustering, the gray scale value of the image pixels is used as feature. Thus the nature of the objective function is of minimization type. The high membership values are assigned to the pixels when gray scale values are close to the centroid of their clusters. The low membership values are assigned to the pixels when the gray scale value is far from the centroid. In FCM algorithm, the degree of membership depends on the distance between the pixel and each individual cluster center. The necessary conditions on u_{ij} and v_i to minimize the objective function (1) are derived by Bezdek [8] as follows:

$$u_{ij} = \frac{\left[\|x_j - v_i\| \right]^{-\frac{1}{m-1}}}{\sum_{k=1}^C \left[\|x_j - v_k\| \right]^{-\frac{1}{m-1}}} \quad (4)$$

$$\text{and } v_i = \frac{\sum_{j=1}^N u_{ij}^m x_j}{\sum_{j=1}^N u_{ij}^m} \text{ for } i = 1, 2, \dots, C, \quad (5)$$

Using iteration technique, the partition memberships and cluster centres are updated to optimize the objective function. Starting with an initial guess for each cluster centre, the iteration processes will be terminated when

$$|J_m^{(k+1)} - J_m^{(k)}| < \epsilon \quad (6)$$

where $0 < \epsilon < 1$ represents the precision of accuracy and k represents the iteration number.

2.2 Introduction to Fuzzy c-means clustering with Spatial Features (FCM_S)

One of the important characteristics of an image is that neighbouring pixels are highly correlated, i.e. the pixels in the immediate neighbourhood possess nearly the same feature data. The probability that they belong to the same cluster is great. So, the spatial relationship of neighbouring pixels is an important characteristic that can be of great aid in image clustering. Utilizing this characteristic in FCM, fuzzy c-means clustering with Spatial Features (FCM_S) was developed (Ahmed, *et al.* [10]). In this method, the spatial information (which is formed by using the distribution statistics of the neighbourhood pixels) and the prior probability are used to form a new membership function for clustering. So in the mathematical structure of the objective function of FCM given in equation (1) is modified as given below:

$$J_u = \sum_{i=1}^C \sum_{j=1}^N u_{ij}^m \|x_j - v_i\|^2 + \frac{\alpha}{N_R} \sum_{i=1}^C \sum_{j=1}^N u_{ij}^m \sum_{x_r \in N_j} \|x_r - v_i\|^2 \quad (7)$$

where α stands for the controlling parameter of the neighbourhood feature,

N_R - the cardinality of the neighbourhood feature,

N_j - the set of neighbours of x_j ,

x_r - the neighbouring data point around x_j falling in the window, with centre x_j .

As in the standard FCM algorithm, the objective is to minimize J_u subject to the constraints on u_{ij} as in the equations (2) and (3). Taking the first derivatives of J_u with respect to u_{ij} and v_i and zeroing them, respectively, two necessary but not sufficient conditions for J_u to be at its local extrema are obtained as follows:

$$u_{ij} = \frac{\left[\|x_j - v_i\|^2 + \frac{\alpha}{N_R} \sum_{x_r \in N_j} \|x_r - v_i\|^2 \right]^{-j}}{\sum_{k=1}^C \left[\|x_j - v_k\|^2 + \frac{\alpha}{N_R} \sum_{x_r \in N_j} \|x_r - v_k\|^2 \right]^{-j}} \quad (8)$$

and
$$v_i = \frac{\sum_{j=1}^N u_{ij}^m \left[x_j + \frac{\alpha}{N_R} \sum_{x_r \in N_j} x_r \right]}{(1 + \alpha) \sum_{j=1}^N u_{ij}^m} \quad (9)$$

2.3 Variations of FCM_S

As FCM_S takes much time for computation, to reduce it, Chen, *et al.* [9] replaced the set of neighbourhood pixels by its mean or median in the equations (7). The objective function is modified as

$$J_u = \sum_{i=1}^C \sum_{j=1}^N u_{ij}^m \|x_j - v_i\|^2 + \alpha \sum_{i=1}^C \sum_{j=1}^N u_{ij}^m \|\bar{x}_j - v_i\|^2 \quad (10)$$

where \bar{x}_j represents the mean in FCM_S₁ and median in FCM_S₂ respectively.

By an optimization way similar to the standard FCM, J_u is minimized under the constraint of U and V same as in equations (4) and (5) are derived as follows:

$$u_{ij} = \frac{[\|x_j - v_i\|^2 + \alpha \|\bar{x}_j - v_i\|^2]^{-\frac{1}{m-1}}}{\sum_{k=1}^C [\|x_j - v_k\|^2 + \alpha \|\bar{x}_j - v_k\|^2]^{-\frac{1}{m-1}}} \quad (11)$$

and
$$v_i = \frac{\sum_{j=1}^N u_{ij}^m [x_j + \alpha \bar{x}_j]}{(1 + \alpha) \sum_{j=1}^N u_{ij}^m} \quad (12)$$

2.4 Introduction to kernelized fuzzy c-means clustering (KFCM)

Euclidean distance (ℓ_2 -norm) is used in FCM, FCM_S and in its variations. So they are not efficient to reveal non-Euclidean structure of the input data. To overcome this disadvantage, a kernelized version of fuzzy-clustering method has been introduced by Chen, *et al.*[9]. The basic idea of kernelizing is, first transforming the low-dimensional inner product input space into a higher dimensional feature space through some nonlinear mapping. Computing a linear partitioning in this feature space results in a nonlinear partitioning in the input space (Chen, *et al.*[9]). By this technique nonlinear structures in input data are preserved after clustering. Chen, *et al.*[9] derived a nonlinear transformation $\Phi: \mathfrak{R}^d \rightarrow \mathfrak{R}^h$ where $d \leq h$, and the metric (norm) is expressed by an inner product space as

$$\|\Phi(v_i) - \Phi(x_j)\|^2 = \langle \Phi(v_i), \Phi(v_i) \rangle + \langle \Phi(x_j), \Phi(x_j) \rangle - 2\langle \Phi(v_i), \Phi(x_j) \rangle.$$

A kernel is defined as

$$K(v, x) = \langle \tau(v_i), \tau(x_j) \rangle = \exp\left(\frac{-\left(\sum_{k=1}^p |v_{ik} - x_{jk}|^a\right)^b}{\sigma^2}\right) \quad (13)$$

where $a \geq 0, 1 \leq b \leq 2$.

By introducing the kernel, the complexity of dimensions in the calculation of the inner products in \mathfrak{R}^h is overcome.

So, $\|\Phi(v_i) - \Phi(x_j)\|^2 = K(v_i, v_i) + K(x_j, x_j) - 2K(v_i, x_j)$ where $i = 1, 2, \dots, C$ and $j = 1, 2, \dots, N$.

As $K(x_i, x_i) = 1$ for any x_i , the above equation can be reformed as

$$\|\Phi(v_i) - \Phi(x_j)\|^2 = 2[1 - K(v_i, x_j)] \quad (14)$$

By using the mapping Φ , the objective function is re written as follows:

$$J_u^{\Phi} = \sum_{i=1}^C \sum_{j=1}^N u_{ij}^m \|\Phi(v_i) - \Phi(x_j)\|^2$$

By introducing this kernel (14), the objective function is modified as,

$$J_u^{\Phi} = \sum_{i=1}^C \sum_{j=1}^N u_{ij}^m [1 - K(v_i, x_j)] \quad (15)$$

The necessary constrains on u_{ij} and v_i for the equation (15) to obtain its local minimum are derived by Chen, *et al.*[9] as follows.

$$u_{ij} = \frac{[1 - K(v_i, x_j)]^{-\frac{1}{m-1}}}{\sum_{k=1}^C [1 - K(v_k, x_j)]^{-\frac{1}{m-1}}} \quad (16)$$

and
$$v_i = \frac{\sum_{j=1}^N u_{ij}^m K(v_i, x_j) x_j}{\sum_{j=1}^N u_{ij}^m K(v_i, x_j)} \quad (17)$$

2.5 KFCM with spatial feature

Analogous to the work in FCM_S, the spatial features are utilized in the KFCM and derived KFCM_S₁, KFCM_S₂ by Chen, *et al.* [9].

The objective function of KFCM with spatial feature (KFCM_S) is defined by Chen, *et al.* [9] as,

$$JS_n^\Phi = \sum_{i=1}^C \sum_{j=1}^N u_{ij}^m [1 - K(v_i, x_j)] + \left(\frac{\alpha}{|N(x_j)|} \right) \sum_{i=1}^C \sum_{j=1}^N u_{ij}^m \sum_{x_r \in N(x_j)} [1 - K(v_i, x_r)] \quad (18)$$

In an analogous way the two necessary conditions on u_{ij} and v_i for the equation (18) to obtain its local minimum are derived by Chen, *et al.*[9]. They are

$$u_{ij} = \frac{\left[[1 - K(v_i, x_j)] + \left(\frac{\alpha}{|N(x_j)|} \right) \sum_{x_r \in N(x_j)} [1 - K(v_i, x_r)] \right]^{\frac{-1}{(m-1)}}}{\sum_{k=1}^C \left[[1 - K(v_k, x_j)] + \left(\frac{\alpha}{|N(x_j)|} \right) \sum_{x_r \in N(x_j)} [1 - K(v_k, x_r)] \right]^{\frac{-1}{(m-1)}}} \quad (19)$$

and

$$v_i = \frac{\sum_{j=1}^N u_{ij}^m \left[K(v_i, x_j) x_j + \left(\frac{\alpha}{|N(x_j)|} \right) \sum_{x_r \in N(x_j)} K(v_i, x_r) x_r \right]}{\sum_{j=1}^N u_{ij}^m \left[K(v_i, x_j) + \left(\frac{\alpha}{|N(x_j)|} \right) \sum_{x_r \in N(x_j)} K(v_i, x_r) \right]} \quad (20)$$

2.6 The variations KFCM_S₁ and KFCM_S₂

To reduce the computational time of KFCM_S, Chen, *et al.*[9] replaced the set of neighboring pixels in equation (18) by its mean or median. The modified objective function is as follows:

$$JS_n^\Phi = \sum_{i=1}^C \sum_{j=1}^N u_{ij}^m [1 - K(v_i, x_j)] + \alpha \sum_{i=1}^C \sum_{j=1}^N u_{ij}^m [1 - K(v_i, \bar{x}_j)] \quad (21)$$

Fuzzy partitioning is carried out through an iterative optimization of the JS_n^Φ with the update of membership u_{ij} and the cluster centres v_i by

$$u_{ij} = \frac{\left[[1 - K(v_i, x_j)] + \alpha [1 - K(v_i, \bar{x}_j)] \right]^{\frac{-1}{(m-1)}}}{\sum_{k=1}^C \left[[1 - K(v_k, x_j)] + \alpha [1 - K(v_k, \bar{x}_j)] \right]^{\frac{-1}{(m-1)}}} \quad (22)$$

and

$$v_i = \frac{\sum_{j=1}^N u_{ij}^m [K(v_i, x_j) x_j + \alpha K(v_i, \bar{x}_j) \bar{x}_j]}{\sum_{j=1}^N u_{ij}^m [K(v_i, x_j) + \alpha K(v_i, \bar{x}_j)]} \quad (23)$$

where \bar{x}_j is the mean and median of the neighbouring pixels within the neighbouring window around x_j in KFCM_S₁ and KFCM_S₂ respectively.

2.7 Some of the disadvantages in using spatial feature

There are two disadvantages in using spatial feature in clustering. They are

- If noise exists in the spatial information, then it will affect the calculations.
- Genuine pixels' gray scale values are changed unnecessarily by adding the spatial feature.

To eliminate the above disadvantages, this article proposes (i) a new mask for spatial feature, (ii) a new "two-phase kernelized fuzzy c-means (TKFCM) algorithm" (iii) a new set of fuzzy rules in defuzzification.

The rest of this paper is organized as follows. In section 3, a “dynamic threshold” is suggested to reduce the noise in the filter widow. In section 4 the new filter window is used as spatial feature in clustering. In section 5 a “two-phase kernelized fuzzy c-means clustering” and new fuzzy rules for defuzzification are introduced. In section 6 the relationship between the methods are discussed. The experimental results are presented in section 7. Section 8 explains the advantages of the above proposed algorithms.

III DYNAMIC SIZED SPATIAL FEATURE WINDOW

For spatial feature in FCM_S, FCM_S₁ and FCM_S₂, a window of neighbouring pixels (generally of size 3x3 or 5x5) around each pixel is used (Ahmed, *et al.* [10]). When any of these neighbouring pixels have noise, it will affect the clustering calculations.

When α -trimmed neighbouring data (Bansal, *et al.* [11], Jampour, *et al.* [12] and Taguchi, *et al.* [13]) are used in the second term of the equations (7) - (12), the sorted neighbouring data are trimmed on both ends equally. Alkhazaleh *et al.* [14] specified that when trimming the neighbouring pixels, if the distribution of neighbouring data is not smooth and having skewness on one side, then the genuine data (without noise) will be trimmed on one end and noisy data will be included on the other end.

Adaptive threshold (dynamic threshold) has been used in recent research works on denoising. (Aborisade [15], Huang *et al.* [16], Sadeghipour [17], Singh [18], Sun *et al.* [19], Yuan *et al.* [20]). But in these articles the entire process is done in wavelet format. Moreover these articles are considering the noise in the central pixel of the spatial window but not in neighbourhood of a pixel. To eliminate the time taken to convert the image to wavelet format, and to eliminate the noise in the spatial information of each pixel x_j , this article proposes a new dynamic threshold which trims the spatial information of each pixel x_j reducing noise. The procedure is explained below:

First, for each pixel value x_j , trimmed mean filter value $\overline{N_T(x_j)}$ is calculated using the equation

$$\overline{N_T(x_j)} = \frac{1}{|N(x_j)| - 2T_s} \sum_{k=T_s+1}^{|N(x_j)| - T_s} x_k \quad (24)$$

where,

$T_s < \frac{|N(x_j)|}{2}$ is an integer representing the “trimming size”

$x_k \in \{N(x_j)\}$ the sorted neighboring pixel of x_j ,

Second, the mean deviation of $T_N(x_j)$ is calculated. It is denoted as σ_j . It is calculated by using the equation

$$\sigma_j = \frac{1}{|N(x_j)|} \sum_{x_k \in N(x_j)} \|x_k - \overline{N_T(x_j)}\|$$

Next by using σ_j as the dynamic threshold, noise less neighbouring pixels are selected by using the equation

$$N_s(x_j) = \{x_k \mid \|x_k - \overline{N_T(x_j)}\| \leq \beta \sigma_j \text{ where } x_k \in N(x_j)\} \quad (25)$$

This set $\{N_s(x_j) \mid j = 1, 2, \dots, N\}$ is proposed to use as spatial information in clustering.

The main concept of this process is, if a pixel, either in centre or in the neighbourhood of the filter window, has noise, it will lie in the region of rejection. The quantity β multiplied with σ_j together with $\overline{N_T(x_j)}$ determines the

region of acceptance. The spatial information of the neighbouring points $\{N_s(x_j)\}$ which are lying within the region of acceptance are taken into account of clustering calculations. The set of points in $\{N_s(x_j)\}$ is called "selected neighbouring pixels". When the median of $N_s(x_j)$ is used as spatial information in clustering, it serves better than median filter value used in Chen, *et al.*[9].

IV HYBRID METHOD OF KFCM WITH SELECTED NEIGHBOURHOOD (KFCM_Ss₂)

4.1 Mathematical model

This method of clustering is based on the Gaussian kernel function. The normed kernel function and the standard objective function of KFCM_S₂ given by Chen, *et al.*[9] are utilized to build the new KFCM_Ss₂. By introducing the new filter window, the objective function given in the equation (21) is modified as

Minimize

$$JS_m^{\#} = \sum_{i=1}^C \sum_{j=1}^N u_{ij}^m [u_{ij}^m [1 - K(v_i, x_j)]] + \alpha \sum_{i=1}^C \sum_{j=1}^N u_{ij}^m [1 - K(v_i, \overline{N_s(x_j)})] \quad (26)$$

Subject to,

$$0 \leq u_{ij} \leq 1 \text{ for } i = 1, 2, \dots, C \text{ and } j = 1, 2, \dots, N$$

$$\sum_{i=1}^C u_{ij} = 1 \text{ for } j = 1, 2, \dots, N$$

where $\overline{N_s(x_j)}$ refers the median of $N_s(x_j)$

An iterative algorithm for minimizing equation (26) with respect to u_{ij} and v_i is derived, as given in (27-28):

$$u_{ij} = \frac{[K(v_i, x_j) + \alpha \sum_j [K(v_i, \overline{N_s(x_j)})]]^{\frac{-1}{m-1}}}{\sum_{k=1}^C [K(v_k, x_j) + \alpha \sum_j [K(v_k, \overline{N_s(x_j)})]]^{\frac{-1}{m-1}}} \quad (27)$$

$$v_i = \frac{\sum_{j=1}^N u_{ij}^m [K(v_i, x_j) x_j + \alpha \sum_j K(v_i, \overline{N_s(x_j)}) \overline{N_s(x_j)}]}{\sum_{j=1}^N u_{ij}^m [K(v_i, x_j) + \alpha \sum_j K(v_i, \overline{N_s(x_j)})]} \text{ for } i = 1, 2, \dots, C, \text{ and } j = 1, 2, \dots, N. \quad (28)$$

4.2 Defuzzification

The output data values are approximated using fuzzy inference formula given below

$$Z = \{z_j \mid z_j = \frac{\sum_{i=1}^C v_i (u_{ij})^m}{\sum_{i=1}^C (u_{ij})^m}\} \quad (29)$$

where $j = 1, 2, N$ and $V' = \{v_1, v_2, \dots, v_C\}$.

V TWO-PHASE KERNELIZED FUZZY C-MEANS CLUSTERING WITH SPATIAL FEATURE (TKFCM_Ss₂)

The proposed method consists of two phases. In phase I, the input image is fuzzified by KFCM. A partition membership matrix $U = [u_{ij}]$ of order $C \times N$ and a set of cluster centers $V = [v_j]$ are calculated. In phase IIa new partition membership matrix $U' = [u'_{ij}]$ of order $C \times N$ and a set of cluster centers $V' = [v'_j]$ are introduced.

U' and V' are initialized by the final iteration values of U and V obtained in phase-I. The image is further fuzzified by KFCM_Ss₂ and the values of U' , V' are calculated by iteration method proposed in section 4.

5.1 Defuzzification

During defuzzification process in KFCM_S₂, the gray scale values of pixels are calculated by fuzzy inference method. This set of gray scale values are an approximation to the original values. There are many defuzzification techniques used in practice (Chaudhuri, *et al.*[21], Roventa[22], Nejad, *et al.*[23], Udupa, *et al.*[24], Sladoje, *et al.*[25], Lowen, *et al.*[26] and Leekwijck, *et al.*[27]), and different rules are applied to find a suitable crisp representation for the fuzzy set.

5.2 Limitations of existing defuzzification methods

In the defuzzification methods referred above, the noise less pixels' gray scale values are unnecessarily changed by inference calculations. The gray scale values in an original crisp image usually match with some physical units in the real world (such as Hounsfield units in computed tomography) or they are relative to some known quantity (e.g., giving the value 0 to water in MRI). Thus, to obtain a better approximation for the original crisp set, defuzzification plays a vital role in fuzzy clustering

To overcome this problem, in this article, a new set of fuzzy rules are proposed for defuzzification. The fact behind this process is that KFCM is more sensitive to noise than KFCM_S₂. It reflects in the corresponding cluster assignment, partition membership values of each pixel (clustered by KFCM and KFCM_S₂). The noise pixels can be identified by comparing the outcomes (i.e. cluster assignment, partition membership and gray scale value calculated by inference method) of KFCM and KFCM_S₂. The difference in the above said outcomes of KFCM and KFCM_Ss₂ of a noisy pixel will be higher than that of its neighboring noiseless pixels. Based on this, the following fuzzy rules are introduced.

If any pixel x_j satisfies at least any one of the following three conditions (i), (ii), and (iii) given in section 5.3 is identified as a noisy pixel, and its fuzzy values are mapped to the spatial feature $N_s(x_j)$.

5.3 Fuzzy rules to identify the noisy pixels

(i) If the pixel assigned to one cluster by KFCM is assigned to some other cluster by KFCM_Ss₂ then the pixel is a noisy pixel.

(ii) If $\|u_{ij} - u'_{ij}\| > \overline{\|N(u_{ij}) - N(u'_{ij})\|}$ then x_j is a noisy pixel,

where

$N(u_{ij})$ is the partition membership value of neighbouring pixels of x_j in cluster i in KFCM.

$N(u'_{ij})$ is the partition membership value of neighbouring pixels of x_j in cluster i in KFCM_Ss₂.

$\overline{\|N(u_{ij}) - N(u'_{ij})\|}$ is the mean of the differences between the partition memberships of neighbouring pixels in KFCM and in KFCM_Ss₂.

(iii) If $\|x_j - z_j\| > \overline{\|N(x_j) - N(z_j)\|}$ then x_j is a noisy pixel,

where $\|N(x_j) - N(z_j)\|$ is the mean of the differences between the neighbouring pixel values in input image and their corresponding inference values in KFCM_Ss₂.

5.4 Proposed Fuzzy rules for defuzzification

The new set of fuzzy rules induces two mappings, one from the fuzzy set to the crisp input set and another from the fuzzy set to the crisp spatial feature set. If the pixel is a noisy pixel, the new set of fuzzy rules constructs an opt mapping from the fuzzy set to the crisp spatial feature set. Otherwise it makes a map from the fuzzy set to the crisp input set. By this proposed method the quantitative features of the pixel value are preserved as in the original noiseless image. In other words, the Peak Signal to Noise Ratio (PSNR) is preserved, and non-Euclidian structures are revealed well when clustering an image. The experiments on synthetic, real and on MR images illustrate that TFCM_Ss₂ is more efficient than the existing fuzzy c-means clustering methods.

5.5 Algorithm for Two-phase Kernelized Fuzzy C-means (TKFCM_Ss₂)

Phase I

Step 1: Get the data from the image.

Step 2: Fix the number of clusters

Step 3: Initialize the cluster centres $V=[v_j]$ using random numbers.

Step 4: Initialize the partition membership matrix $U=[u_{ij}]$ where $i = 1, 2 \dots C, j = 1, 2 \dots N$ by random numbers satisfying the equations (2) and (3).

Step 5: Fix the precession value $\epsilon, (0 < \epsilon < 1)$.

Step 6: Update the partition membership matrix $U=[u_{ij}]$ using the equation (16).

Step 7: Update the prototype centres $V=[v_j]$ using the equation (17).

Step 8: Calculate the value of the objective function J_m using the equation (15).

Step 9: Repeat steps from (5) to (7) until $|J_m^{(k+1)} - J_m^{(k)}| < \epsilon$ is satisfied, where $J_m^{(k)}$ and $J_m^{(k+1)}$ are the values of the objective function obtained in the k^{th} and $(k+1)^{th}$ iterations respectively.

Phase II

Step 1: Initialize the new partition membership matrix $U'=[u'_{ij}]$ and the cluster centre $V'=[v'_j]$ of phase II with the final values of U and V respectively obtained from the step 9 in phase I.

Step 2: Initialize the controlling parameter $\alpha (0 < \alpha < \infty)$ in the neighbourhood feature.

Step 3: Fix a (3x3) neighbourhood window on each pixel $x_j (j = 1, 2 \dots N)$ with x_j as the centre of the window.

Step 4: Update the partition membership matrix U' by giving modification (i.e. replacing u_{ij} by u'_{ij}) in equation (27).

Step 5: Update the prototype V' by giving modification (i.e. replacing v_j by v'_j) in equation (28).

Step 6: Calculate the value of the objective function J_m^s using the equation (26).

Step 7: Repeat steps from (12) to (14) until $|J_m^{s(k+1)} - J_m^{s(k)}| < \epsilon$ is reached, where $J_m^{s(k)}$ and $J_m^{s(k+1)}$ are the values of the objective function obtained in k^{th} and $(k+1)^{th}$ iterations respectively.

5.6 Algorithm for defuzzification using the proposed fuzzy rules

Step 1: Create two binary matrices B and B' of same order $(C \times N)$, with

$$B_{ij} = \begin{cases} 1 & \text{if } x_j \text{ has maximum membership in } i^{\text{th}} \text{ cluster of } U, \\ 0 & \text{otherwise} \end{cases}$$

and $B'_{ij} = \begin{cases} 1 & \text{if } x_j \text{ has maximum membership in } i^{\text{th}} \text{ cluster of } U', \\ 0 & \text{otherwise} \end{cases}$

Step 2: Calculate the set Z of inference values by using the equation (29)

$$Z = \left\{ z_j \mid z_j = \frac{\sum_{i=1}^C v'_i (u'_{ij})^m}{\sum_{i=1}^C (u'_{ij})^m} \right\}$$

where $j = 1, 2, \dots, N$ and $V' = \{v'_1, v'_2, \dots, v'_C\}$ obtained from the modified equation used in step (5) of phase II in section (5.5).

Step 3: Construct the new crisp set $\{y_j\}$ as

$$y_j = \begin{cases} x_j & \text{if } B_{ij} \text{ and } B'_{ij} \text{ are equal,} \\ \overline{N_s(x_j)} & \text{otherwise.} \end{cases} \quad \text{for } i = 1, 2, \dots, C \text{ and } j = 1, 2, \dots, N.$$

where $\overline{N_s(x_j)}$ is the median of the selected neighbourhood pixels of x_j .

Step 4: Convert U and U' into three dimensional matrices of order (C, H, W) ,

Convert $\{y_j\}$ and $\{z_j\}$ into (H, W) matrix, where H, W is the height and width of the input image.

Step 5: If $|u_{i,k,q} - u'_{i,k,q}| > \overline{|u_{i,k,q} - u'_{i,k,q}|}$ then $y_{k,q} = \overline{N_s(x_{k,q})}$

where $\overline{|u_{i,k,q} - u'_{i,k,q}|}$ is the mean of the set of absolute differences $\{|N(u_{i,k,q}) - N(u'_{i,k,q})|\}$

$$i = 1, 2, \dots, C, \quad k = 1, 2, \dots, H, \quad q = 1, 2, \dots, W$$

Step 6: Fix $N(z_{k,q})$ and $N(y_{k,q})$ for $k = 1, 2, \dots, H, \quad q = 1, 2, \dots, W$

Step 7: Calculate $|N(z_{k,q}) - N(y_{k,q})|$

$$\text{If } |z_{k,q} - y_{k,q}| \geq \overline{|N(z_{k,q}) - N(y_{k,q})|} \text{ then } y_{k,q} = \overline{x_{k,q}}$$

where $\overline{|N(z_{k,q}) - N(y_{k,q})|}$ is the mean of the set of absolute differences $\{|N(z_{k,q}) - N(y_{k,q})|\}$

Step 8: Assign $y_{k,q}$ to the cluster in which $x_{k,q}$ has maximum membership value in U' for $k = 1, 2, \dots, H, q = 1, 2, \dots, W$.

VI RELATIONSHIP AMONG THE VARIOUS METHODS.

Two phase fuzzy c-means clustering algorithm can be considered as a general framework. Besides TKFCM_Ss₂, some other typical clustering algorithms for image clustering can be derived from the framework as follows:

1) By setting $\overline{N_s(x_j)}$ as the mean of $N_s(x_j)$ in equations (26), (27) and (28), the KFCM_Ss₂ reduces to KFCM_Ss₁.

Similarly TKFCM_Ss₂ reduces into TKFCM_Ss₁.

- 2) By replacing $N(x_j)$ with $N_s(x_j)$ in equations (19), (20), and (21) and replacing the equations (26), (27), (28) with the modified form of equations (19), (20), and (21), KFCM_Ss₂ reduces to KFCM_Ss. In an analogous way TKFCM_Ss₂ reduces to TKFCM_Ss.
- 3) When $\beta \rightarrow \infty$ in equation (24), $N_s(x_j) \rightarrow N(x_j)$. Then KFCM_Ss₂ reduces into KFCM_S₂, and TKFCM_Ss₂ becomes TKFCM_S₂ which is a special case of two-phase clustering.
- 4) By setting the trimming size $T_s=0$, in equation (24), KFCM_Ss₂ reduces to KFCM_S₂ and TKFCM_Ss₂ reduces to TKFCM_S₂.

VII EXPERIMENT RESULTS AND ANALYSIS

This section compares the efficiency of the proposed algorithms TKFCM_Ss₂ and KFCM_Ss₂, with KFCM_S₁ (with α -trimmed mean), and KFCM_S₂ on synthetic, real and simulated MR images. The results are graded by measuring the Segmentation Accuracy (S.A) and Peak Signal to Noise Ratio (PSNR), and the number of misclassified pixels. As FCM, FCM_S₁, FCM_S₂, KFCM_S₁ are inferior to KFCM_S₁ (with α -trimmed mean), and KFCM_S₂ they are not used for comparison. To provide the best methods only, here the new variations KFCM_Ss, KFCM_Ss₁, TKFCM_Ss, and TKFCM_Ss₁ are not used for comparison as they are performing inferior to TKFCM_Ss₂ and TKFCM_Ss₂.

7.1 Segmentation Accuracy (S.A.)

The Segmentation Accuracy is calculated as $S_{ij} = \frac{A_{ij} \cap A_{refj}}{A_{ij} \cup A_{refj}}$

where A_{ij} refers the set of pixels of the j^{th} cluster found by the i^{th} algorithm, and A_{refj} represents the set of pixels of the j^{th} cluster in the reference (original) segmented image.

7.2 Peak Signal to Noise Ratio (PSNR)

When spatial feature is used in clustering, even though the S.A. is increased, the output clusters are blurred. So S.A. is not the only scale to measure the quality of clustering. PSNR is an approximation to human perception of reconstruction quality. PSNR is generally used to measure the quality of reconstruction from the noisy data. Higher PSNR indicates that the reconstruction is of higher quality. It is calculated in decibels (dB) and is defined via the mean squared error (MSE) as follows:

If X is the noise-free ($H \times S$) monochrome image, and Y is the output from the noise induced version then, the MSE is given by the equation

$$MSE(X, Y) = \frac{1}{T * S} \sum_{i=1}^T \sum_{j=1}^S |x_{ij} - y_{ij}|^2$$

and the PSNR is calculated as $PSNR = 20 \log_{10} \left(\frac{2^B - 1}{\sqrt{MSE}} \right)$

where B represents the bits per sample pixel. In 8-bit synthetic and real images $B = 8$, in dicom format MRI, it is 16. In the present experiments the PSNR value is calculated for the sum of the clusters.

7.3 Parameter settings

In fact, all these algorithms have some crucial parameters needed to be adjusted for clustering and the parameters are noise dependent. Therefore their selection will trivially influence the clustering results. This section focuses on discussion on the parameter setting.

In all these experiments the parameters are set as follows: $m = 2$, $\epsilon = 0.00001$. The algorithms are tested on images corrupted by “Gaussian”, “Salt & Pepper” and “Mixed” noises respectively.

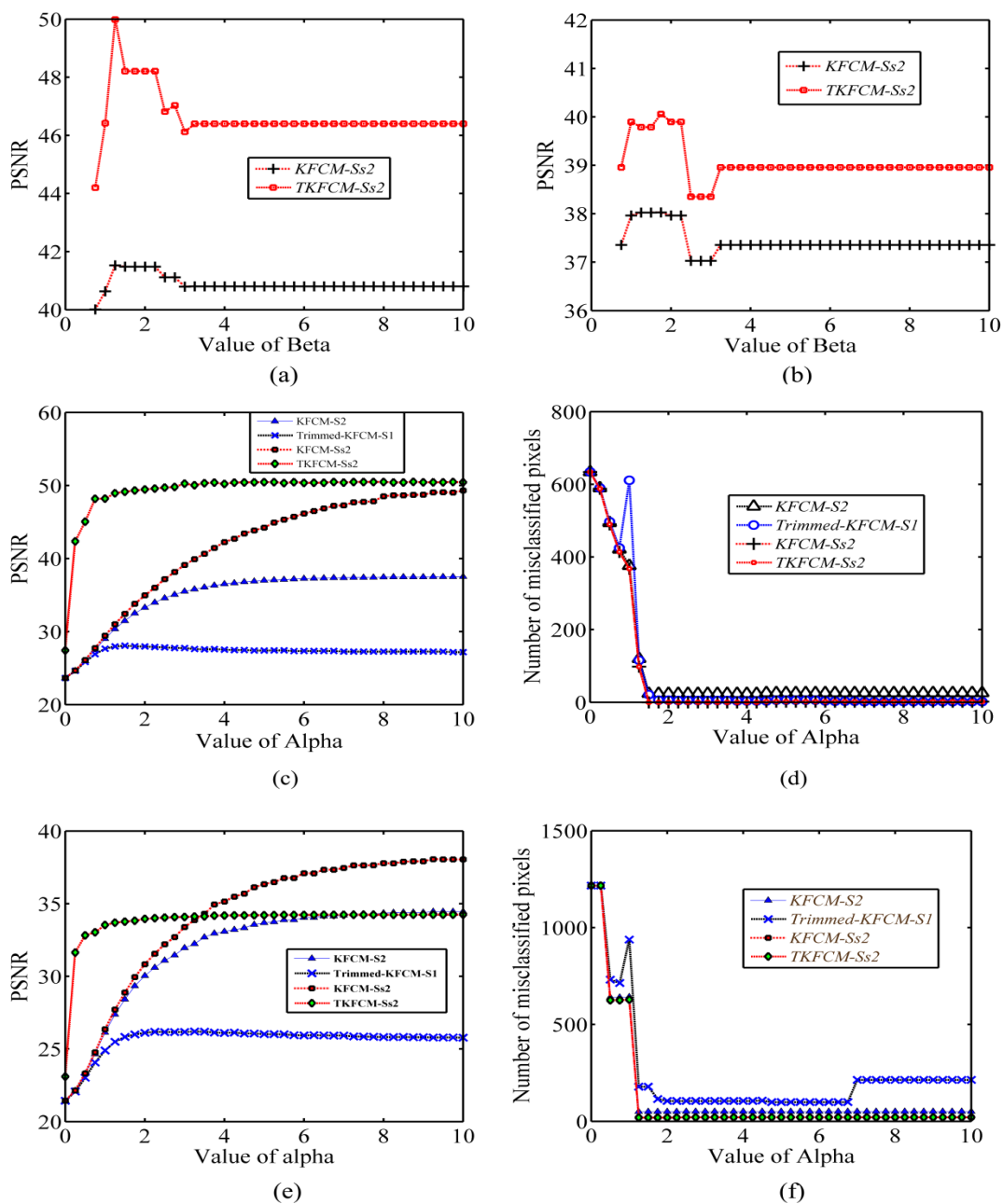
7.4. Results on synthetic image

A synthetic image of size [128x128] pixels includes two classes of grey values {0, 90} is used for this experiments.

7.4.1 The first experiment is conducted to test the effect of β in PSNR of output clusters. In this experiment β is assigned values 0.75 through 10 in steps of 0.25. Fig.(1a) and (1b) show the PSNR of results of KFCM_Ss₂, and TKFCM_Ss₂ varying with the parameter β on the synthetic image corrupted by Gaussian” and “Salt & Pepper” noise respectively. Similar result is obtained in the case of mixed noise. As there is no significant change in the clustering performance after $\beta = 3.5$ the value of β is set as 3.5 in equation (24) for the second and third experiments.

7.4.2 The second experiment is conducted on synthetic image to test the effect of various values for the parameter α in segmentation performance. In this experiment α is assigned values 0 through 10 in steps of 0.25. The results of the proposed methods are compared with the existing methods KFCM_S₁ (with α -trimmed mean) and KFCM_S₂. The result is presented in Fig. (1c) and in Fig.(1d). The results show that the segmentation performance is varying with the value of α . As there is no significant change in the clustering performance after $\alpha = 3.8$ the value of α is set as 3.8 for third experiments. In the first and second experiments, the noise level is fixed as 10%.

7.4.3. The third experiment is conducted on synthetic image to compare the PSNR together with classification errors in the results obtained by KFCM_S₁ (with α -trimmed mean), KFCM_S₂, KFCM_Ss₂, and TKFCM_Ss₂. The value of α is fixed as 3.8 (the optimal value used in Chen, *et al.*[9]) and C as 2. The noise level is set at various levels ranging from 3% through 15%. “Gaussian”, “Salt & Pepper” and “Mixed noises” are used. Simulation of noise was performed by 100 independent runs on each level and each type of noise. The simulated different structures of noise in synthetic image are tested by KFCM_S₁ (with α -trimmed mean), KFCM_S₂, KFCM_Ss₂, and TKFCM_Ss₂. The average segmentation accuracy and average PSNR% are presented in Table (1). The graphical representations of the results are given in Fig.(1.e) and Fig.(1.f). From the results it is observed that as noise level increases the clustering performance is decreasing. But in all the cases KFCM_Ss₂ and TKFCM_Ss₂ is performing better than KFCM_S₁ (with α -trimmed mean) and KFCM_S₂. The output images are presented in Fig. (2).



Fig(1). Graphical representation of effect of parameters in synthetic image clustering.

- (a) Comparison of PSNR on synthetic image with Gaussian noise under different values of β .
- (b) Comparison of PSNR on synthetic image with salt and pepper noise under different values of β .
- (c) Comparison of PSNR on synthetic image with Gaussian noise under different values of α .
- (d) Comparison of classification errors on synthetic image with Gaussian noise under different values of α .
- (e) Comparison of PSNR on synthetic image with salt and pepper noise under different values of α .
- (f) Comparison of classification errors on synthetic image with salt and pepper noise under different values of α .

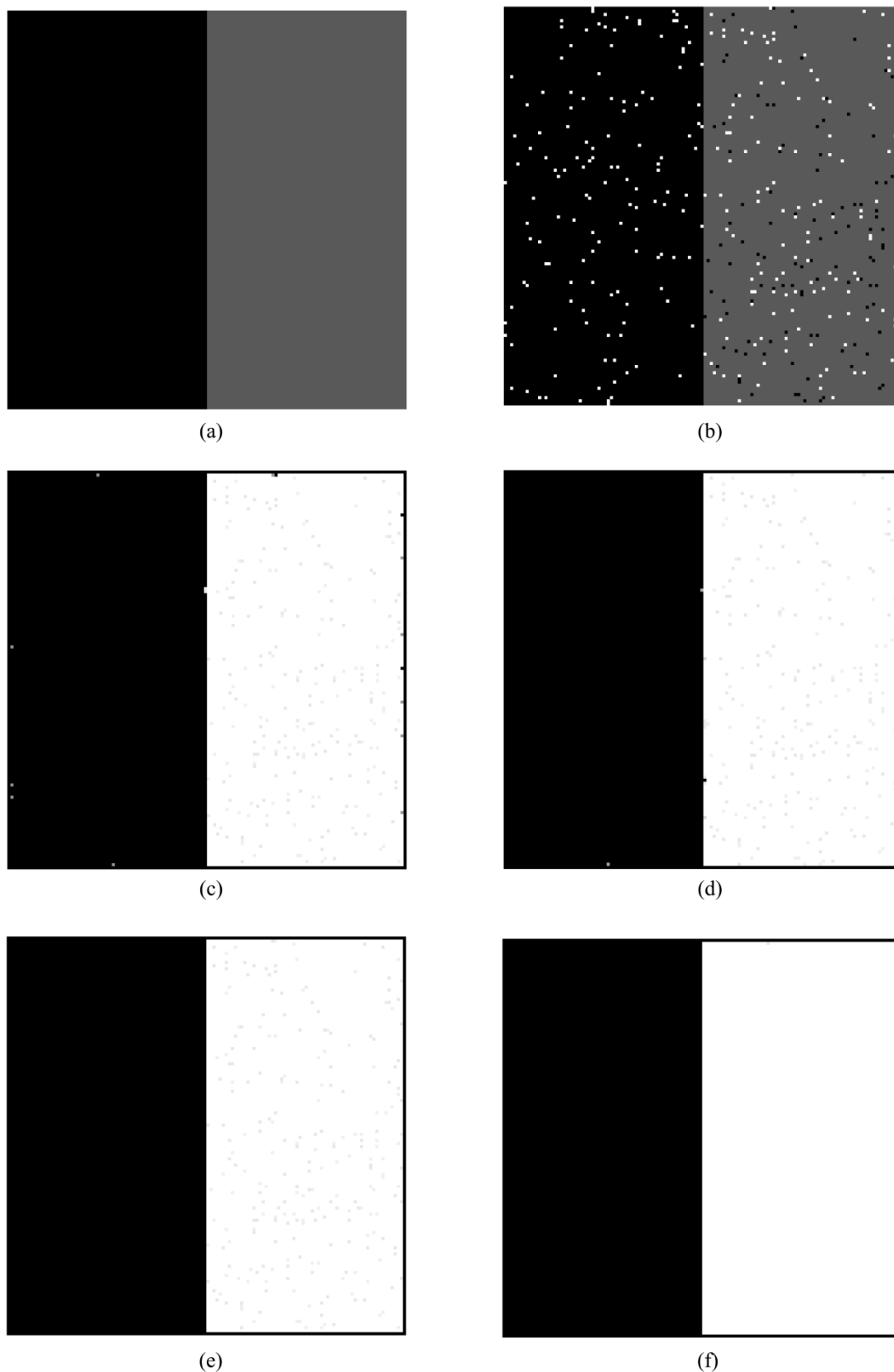


Fig (2). Comparison of segmentation results of synthetic image.

(a) Original image, (b) image with 'Salt & Pepper' noise, (c) KFCM_S2 result, (d) KFMC_S1 (with Trimmed mean) result, (e) KFCM_Ss2 result, (f) TKFCM_Ss2 result.

7.5. Experiment on real image

To examine the robustness of the algorithms, the real image “eight” of size 242 x 308 with gray values 0 to 255 corrupted simultaneously by Gaussian white noise $N(0,180)$ with unit dispersion, and salt & pepper noise. There are three types of experiments conducted on the experimental object.

7.5.1 The first experiment is conducted on real image to test the effect of various values for the parameter β in segmentation performance. The graphical representation of the results are presented in Fig.(3.a) show that the PSNR of the output of KFCM_Ss₂, and TKFCM_Ss₂ is varying with the parameter β . As there is no significant change in the clustering performance after $\beta = 3.5$ the value of β is set as 3.5 in equation (24) for the second and third experiments.

7.5.2 The second experiment is conducted on real image to test the effect of various values for the trimming size (T_s) in segmentation performance. As a 3x3 window is used for spatial feature, the trim size T_s in equation (24) can be assigned as $T_s \in \{0,1,2,3,4\}$. The graphical representation of the segmentation performance is presented in Fig.(3b). From the results, it is observed that when $T_s = 3$ the algorithms KFCM_Ss₂ and TKFCM_Ss₂ are reaching their maximum performance.

7.5.3. The third experiment is conducted on real image to compare the segmentation performance of the proposed methods with existing methods. The PSNR and the classification errors in the results obtained by KFCM_S₁ (with α -trimmed mean), KFCM_S₂, KFCM_Ss₂ and TKFCM_Ss₂ are compared. The value of α is fixed as 3.8 (the optimal value used in Chen, *et al.*[9] β as 3.5, T_s as 3 and C as 2. The PSNR and segmentation accuracy are presented in Table (1), and the graphical representation of the results are given in Fig.(3.c) and Fig.(3.d). From the results it is realized that KFCM_Ss₂ and TKFCM_Ss₂ are performing better than KFCM_S₁ (with α -trimmed mean) and KFCM_S₂. The output images are given in Fig.(4). As the existing defuzzification method is used in KFCM_S₁ (with α -trimmed mean), KFCM_S₂ and KFCM_Ss₂ the output images lose their clarity. But as the proposed “two-phase defuzzification” is used in TKFCM_Ss₂, the defuzzified image has better clarity and revealing non-Euclidean structures well in the output clusters (please zoom in the image to see). Similar performances are obtained in the case of “Gaussian” and “Salt & Pepper” noised images.

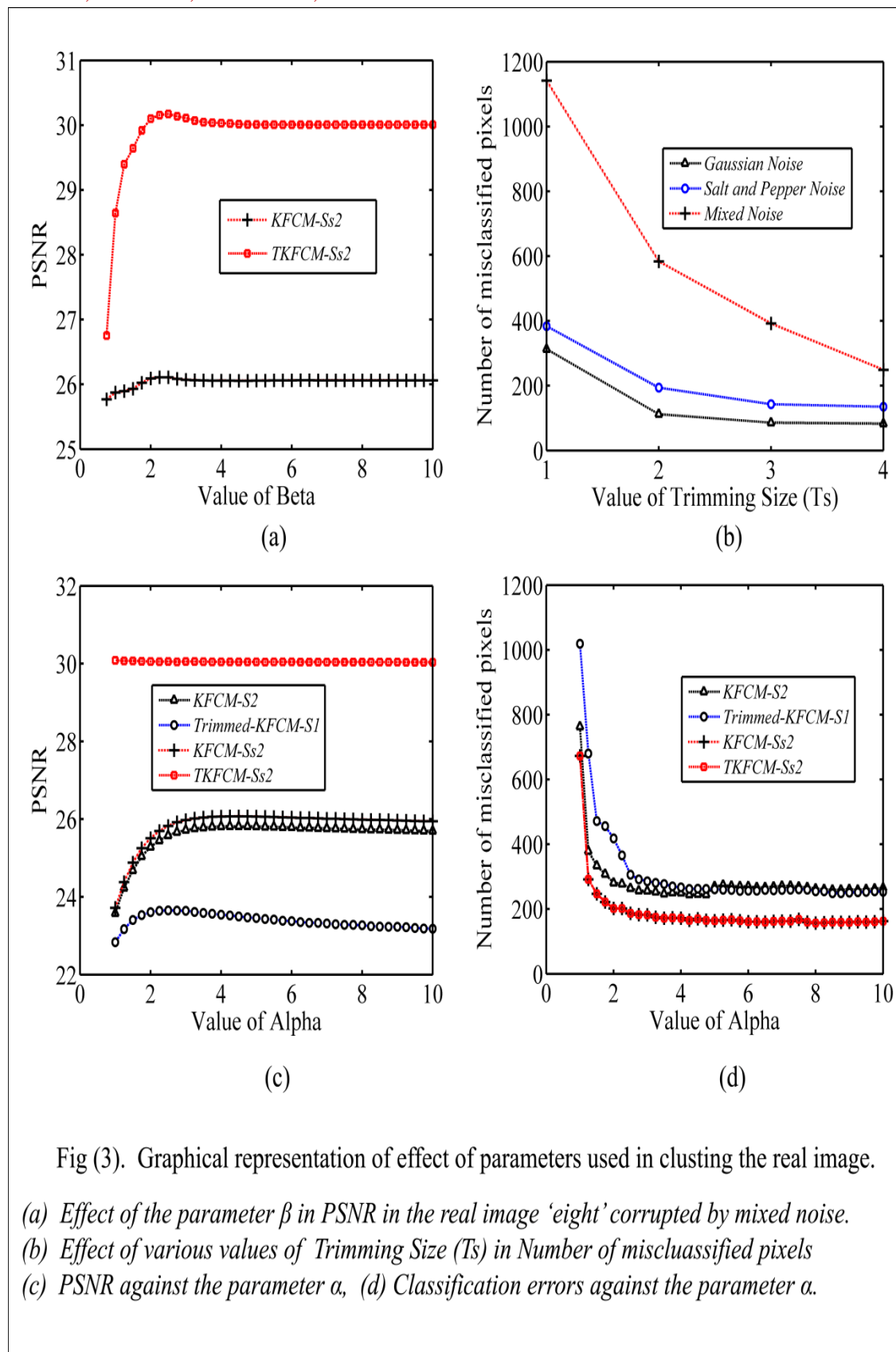
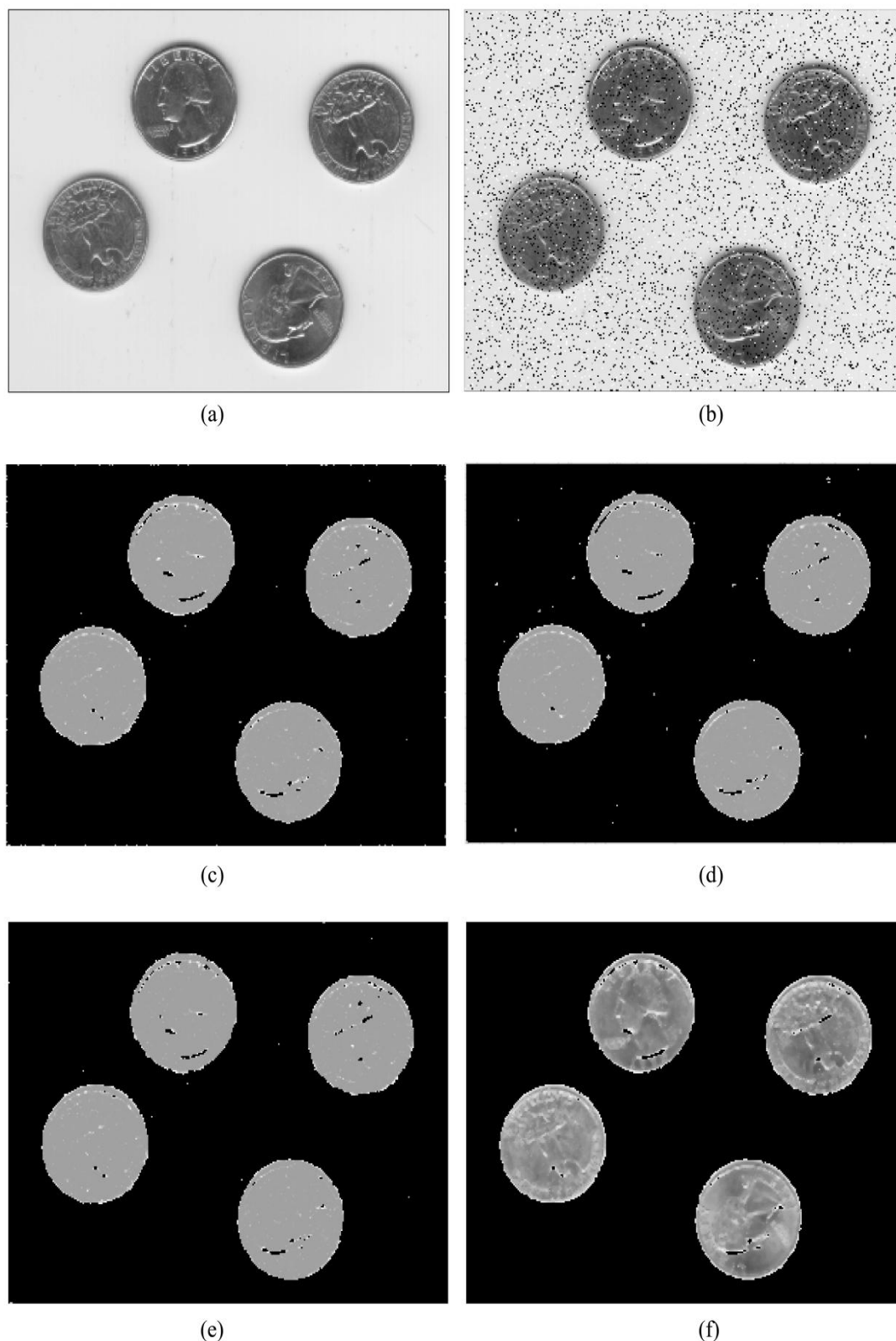


Fig (3). Graphical representation of effect of parameters used in clustering the real image.

- (a) Effect of the parameter β in PSNR in the real image 'eight' corrupted by mixed noise.
- (b) Effect of various values of Trimming Size (T_s) in Number of misclassified pixels
- (c) PSNR against the parameter α , (d) Classification errors against the parameter α .



Fig(4) Comparison of clustering results of real image.

(a) Original image, (b) image with mixed noise with $r = 0.5$, (c) KFCM_S2 result, (d) KFMC_S1 (with Trimmed mean) result, (e) KFCM_Ss2 result, (f) TKFCM_Ss2 result.

7.6. Experiments on simulated MRI

In this experiment, a high-resolution T1-weighted simulated phantom image (used in Cai et al. [28]) with 181×181 pixels, 1 mm slice thickness, 9% Gaussian noise and no gray inhomogeneous is used as experimental object. The slice is in the axial plane with sequence 91. In nature, the MRIs are not affected by Gaussian noise. But it is added for experimental purpose.

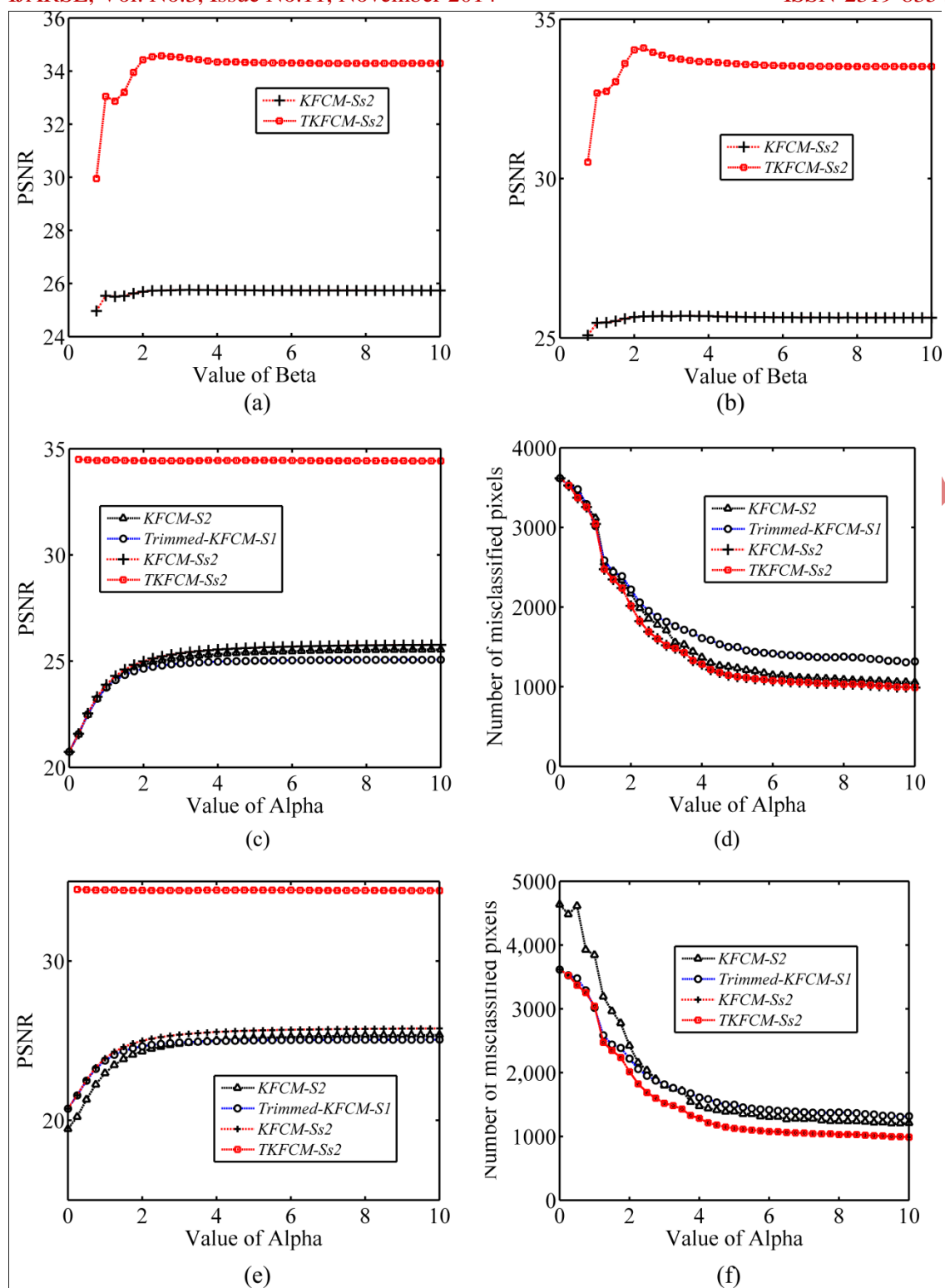
In an analogous way the first two types of experiments are conducted to test the effect of various values of β and α in segmentation performance. The graphical results are presented in Fig.(5.a), (5.c) and (5.d). Similar result obtained in the case of salt & pepper noise is presented in Fig.(5.b), (5.e) and (5.f).

7.6.1 Third experiment on Simulated MRI

In this experiment the PSNR and the classification errors in the results obtained by KFCM_S₁ (with α -trimmed mean), KFCM_S₂, KFCM_Ss₂, and TKFCM_Ss₂ are compared. For this experiment the parameter α is set as 9 (the optimal value used in Chen, et al. [9]), β as 3.5 and C as 3. The output images are presented in Fig. (6).

As the existing defuzzification method is used with KFCM_S₁ (with α -trimmed mean) KFCM_S₂, KFCM_Ss₂, the image loses its clarity and non-Euclidean structures are not revealed well and they have low PSNR values. But when the proposed “two-phase defuzzification” is used in TKFCM_Ss₂, the defuzzified image is very similar to the original noiseless image and the PSNR is increased.

For Gaussian and Salt & Pepper noised images, the quantitative comparisons of “selected neighbourhood pixels” with the existing neighbourhood masks are presented in Table (1). From the figures and Table values “selected neighbourhood pixels” produce better segmentation accuracy and “two-phase defuzzification methods” is giving higher PSNR values than the corresponding existing defuzzification methods. The effect is reflecting in the output figures.



Fig(5). Graphical representation of effect of parameters used in clustering the simulated MRI.
 (a) β vs PSNR_in simulatedMRI corrupted by Gaussian noise.
 (b) β vs PSNR_in simulated MRI corrupted by Salt & Pepper noise.
 (c) α vs PSNR in simulatedMRI corrupted by Gaussian noise.
 (d) α vs MissClassification_in simulated MRI corrupted by Gaussian noise.
 (e) α vs PSNR in simulatedMRI corrupted by Salt & Pepper noise.
 (f) α vs MissClassification_in simulated MRI corrupted by Salt & Pepper noise.

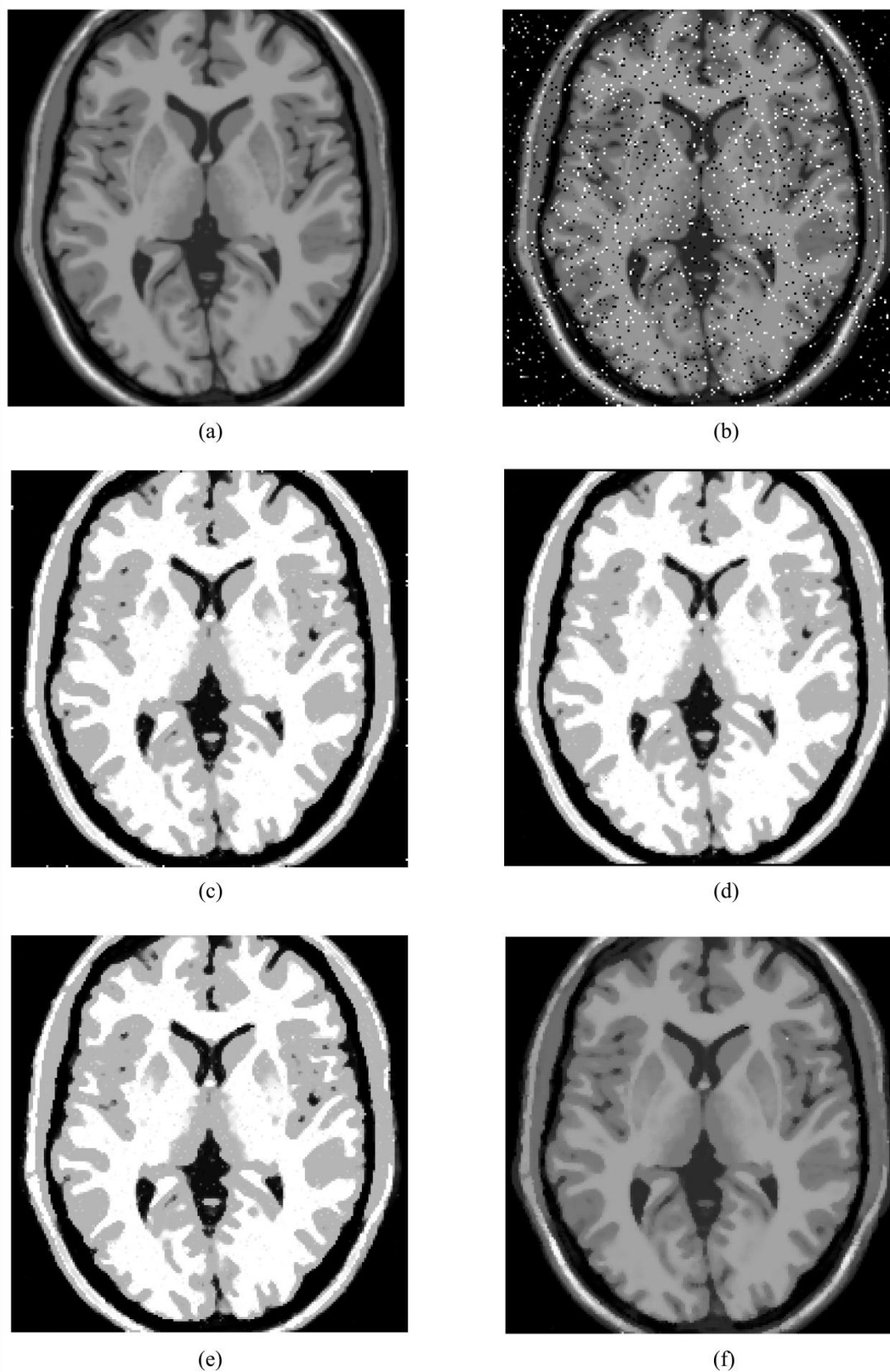


Fig (6). Comparison of defuzzification results of Simulated Brain image.

(a) Original image, (b) image with '9% Gaussian noise, (c) KFCM_S2 result, (d) KFMC_S1 (with Trimmed mean) result, (e) KFCM_Ss2 result, (f) TKFCM_Ss2 result.

VIII CONCLUSION

From the figures and table values “selected neighbourhood masks” produce better segmentation accuracy and “two-phase defuzzification method” is giving higher PSNR values than the corresponding existing defuzzification methods in synthetic, real and simulated MR images and the effect is reflecting in the output figures.

Table 1
Comparison of segmentation performance of clustering methods

Noise Type and level (%)		Existing Methods						Proposed Methods					
		KFCM_S ₁ (Trimmed Mean)			KFCM_S ₂			KFCM_S _{s2}			T KFCM_S _{s2}		
		PSNR	No. of Misclassified	S.A	PSNR	No. of Misclassified	S.A	PSNR	No. of Misclassified	S.A	PSNR	No. of Misclassified	S.A
Synthetic Image													
Gaussian	3%	27.66	1	0.9999	42.52	5	0.9994	47.44	0	1.0000	63.51	0	1.0000
	5%	27.62	1	0.9999	39.38	12	0.9985	43.58	2	0.9998	49.49	2	0.9998
	8%	27.52	5	0.9994	37.09	22	0.9973	40.02	8	0.9990	42.23	8	0.9990
	10%	27.51	4	0.9995	36.33	24	0.9971	40.81	2	0.9998	46.30	2	0.9998
Salt & Pepper	3%	27.61	3	0.9996	40.29	10	0.9988	42.89	2	0.9998	48.13	2	0.9998
	5%	27.44	9	0.9989	38.43	14	0.9983	42.89	2	0.9998	48.08	2	0.9998
	10%	27.12	21	0.9974	34.21	40	0.9951	37.36	10	0.9988	41.01	10	0.9988
	15%	26.15	105	0.9873	32.96	51	0.9938	34.85	22	0.9973	35.51	22	0.9973
Mixed noise	r=0.3	25.01	1	0.9998	26.14	8	0.9990	29.26	0	1.0000	29.21	0	1.0000
	r=0.5	22.23	3	0.9996	24.37	8	0.9989	24.64	1	1.0000	24.51	1	1.0000
	r=0.7	20.32	5	0.9994	20.49	9	0.9989	20.52	1	0.9999	20.54	1	0.9999
Real Image													
Mixed noise r=0.5		23.58	313	0.9916	25.90	244	0.9935	26.13	165	0.9956	30.18	165	0.9956
Simulated MRI													
Gaussian 9%		25.06	1346	0.9719 0.9597 0.9875	25.51	1072	0.9786 0.9687 0.9881	25.72	1012	0.9744 0.9621 0.9873	34.45	1012	0.9803 0.9696 0.9891

REFERENCES

- [1] Yong, Y., Chongxun, Z. and Pan, L. (2004). A novel fuzzy c-means clustering algorithm for image thresholding. *Measurement Science Review*, 4(1), pp.11-19.
- [2] Pham, D.L, Xu, C.Y., and Prince, J. L (2000). A survey of current methods in medical image segmentation. *Annual Review of Biomedical Engineering*, 2, pp.315-337.
- [3] Bezdek, J.C., Hall, L.O, and Clarke, L.P (1993). Review of MR image segmentation techniques using pattern recognition. *Medical Physics*, 20(4), pp.1033 -1048
- [4] Wells III,W.M., Grimson,W.E.L, Kikinis, R. and Jolesz, F. A. (1996). Adaptive segmentation of MRI data. *Medical Imaging, IEEE Transactions*, 15(4), pp.429-442.
- [5] Pham, D.L. and Prince, J.L (1999). An adaptive fuzzy C means algorithm for image segmentation in the presence of intensity inhomogeneities. *Pattern Recognition Letters*, 20(1), pp.57-68.
- [6] Zadeh, L. (1965). Fuzzy sets. *Information and control*, 8(3), pp.338-353.
- [7] Dunn, J.C (1974). A Fuzzy Relative of the ISODATA Process and its Use in Detecting Compact Well Separated Clusters. *Journal of Cybernetics*, 3, pp.32-57.
- [8] Bezdek, J.C (1981). *Pattern recognition with fuzzy objective function algorithms* 1st ed. New York: Plenum Press.
- [9] Chen, S.C. and Zhang, D.Q (2004). Robust image segmentation using FCM with spatial constraints based on new kernel-induced distance measure. *Systems, Man, and Cybernetics, Part B: Cybernetics, IEEE Transactions on*, 34(4), pp.1907-1916.
- [10] Ahmed, M.N., Yamany, S.M., Mohamed, N., Farag, A.A. and Moriarty, T.(2002). A modified fuzzy c-means algorithm for bias field estimation and segmentation of MRI data. *Medical Imaging, IEEE Transactions*, 21(3), pp.193-199.
- [11] Bansal, R., Sehgal, P., and Bedi, P. (2007). A Simplified Fuzzy Filter for Impulse Noise Removal using Thresholding. *ICSPIE in the World Congress on Engineering and Computer Science, San Francisco, USA*.
- [12] Jampour, M., Ziari, M., Zadeh, R. and Ashourzadeh, M. (2010). Impulse noise detection and reduction using fuzzy logic and median heuristic filter. *Networking and Information Technology (ICNIT), International Conference*. pp. 19-23. IEEE.
- [13] Taguchi, A. (1995). An adaptive α -trimmed mean filter with excellent detail-preservation and evaluation of its performance. *Electronics and Communications in Japan (Part III: Fundamental Electronic Science)*, 78(10), pp.46-56.
- [14] Alkhazaleh, A.M.H. and Razali, A.M. (2010). New Technique to Estimate the Asymmetric Trimming Mean. *Journal of Probability and Statistics*, 2010, pp.1-9.
- [15] Aborisade, D.O (2011). A Novel Fuzzy logic Based Impulse Noise Filtering Technique. *International Journal of Advanced Science and Technology*, 32, pp.79-88.
- [16] Huang, B. and Jiao, Y. (2014). A New Adaptive Threshold Image-Denoising Method Based on Edge Detection. *TELKOMNIKA Indonesian Journal of Electrical Engineering*, 12(5), pp.3509-3514.
- [17] Sadeghipour, Z., Babaie-Zadeh, M. and Jutten, C. (2009). An adaptive thresholding approach for image denoising using redundant representations. *Machine Learning for Signal Processing, MLSP 2009. IEEE*

International Workshop, pp.1-6. IEEE

- [18] Singh, K.M (2011). Fuzzy rule based median filter for gray-scale images. *Journal of information Hiding and Multimedia signal processing*, 2(2), pp.108-122.
- [19] Sun, H., Li, K., Wang, H., Chen, P. and Cao, Y. (2014). Intelligent Mechanical Fault Diagnosis Based on Multiwavelet Adaptive Threshold Denoising and MPSO. *Mathematical Problems in Engineering*.
- [20] Yuan, L., Wu, J. and Li, S. (2014). Improved Wavelet Threshold for Gray Scale Image Denoising. *International Journal of Signal Processing, Image Processing and Pattern Recognition*, 7(3), pp.45-52.
- [21] Chaudhuri, B.B. and Rosenfeld, A. (1996). On a metric distance between fuzzy sets. *Pattern Recognition Letters*, 17(11), pp.1157-1160.
- [22] Roventa, E. and Spircu, T. (2003). Averaging procedures in defuzzification processes. *Fuzzy Sets and Systems*, 136(3), pp.375-385.
- [23] Nejad, H.V., Pourreza, H.R. and Ebrahimi, H. (2006). A novel fuzzy technique for image noise reduction. *Transactions on Engineering, Computing, and Technology, Enformatika*, 14, pp.390-395.
- [24] Udupa, J.K. and Samarasekera, S. (1996). Fuzzy connectedness and object definition: theory, algorithms, and applications in image segmentation. *Graphical models and image processing*, 58(3), pp.246-261.
- [25] Sladoje, N., Lindblad, J. and Nystrom, I. (2011). Defuzzification of spatial fuzzy sets by feature distance minimization. *Image and Vision Computing*, 29(2), pp.127-141.
- [26] Lowen, R. and Peeters, W. (1998). Distances between fuzzy sets representing grey level images. *Fuzzy sets and Systems*, 99(2), pp.135-149.
- [27] Leekwijck, W.V and Kerre, E. (1999). Defuzzification: criteria and classification. *Fuzzy sets and systems*, 108(2), pp.159-178.
- [28] Cai, W., Chen, S. and Zhang, D. (2007). Fast and robust fuzzy c means clustering algorithms incorporating local information for image segmentation. *Pattern Recognition*, 40(3), pp.825-838.



Dr.K.Kadambavanam was born in Palni, Tamilnadu, India in 1956.He did his post-graduate studies at Annamalai University, Tamil Nadu, India in 1979. He completed his M.Phil. degree in Annamalai University in 1981. He obtained his Ph.D., degree from Bharathiar University, Coimbatore, Tamil Nadu, India. His area of research is Fuzzy Queueing Models and Fuzzy Inventory Models. His research interests include Solid mechanics, Random Polynomials and Fuzzy Clustering. He has 33 years of teaching experience in both U.G and P.G level and 18 years of research experience. He is a Chairman of Board of Studies (P.G) in Mathematics and Ex-Officio Member in Board of Studies (U.G) in Mathematics in Bharathiar University, Coimbatore. He is a member in : Panel of Resource Persons, Annamalai University, Annamalai Nagar, Doctorial Committee for Ph.D., program, Gandhigram Rural University, Gandhigram.



T. Senthil nathan is an Associate Professor in Post Graduate and Research Department of Mathematics, Erode Arts and Science College, Erode, Tamil Nadu,

India. He received M.Sc. from Periyar E.V.R College, Trichy, Tamil Nadu, and M.Phil. from A.V.V.M. Sri.Pushpam College, Tanjavour, Tamil Nadu, India in 1985 and 1987 respectively. He received M.S. (software) from Birla Institute of Technology and Science (BITS), Pilani, India in 1994. He has 25 years of experience in teaching. He is a member in Board of Studies (U.G. and P.G.) in Mathematics in Erode Arts and Science College. Her research interests include image processing, signal processing, fuzzy logic and its application.

IJARSE